Supplementary Information for

Adsorption and desorption mechanisms of rare earth elements (REEs) by layered double hydroxide (LDH) modified with chelating agents

Shuang Zhang [1, 2], Naoki Kano [3, *], Kenji Mishima [4, 5], Hirokazu Okawa [6]

1. Jiangxi Province Key Laboratory of Polymer Micro/Nano Manufacturing and Devices, East China University of Technology, Nanchang, 330013, People's Republic of China; zs6261@163.com
2. Graduate School of Science and Technology, Niigata University, 8050 Ikarashi 2-Nocho, Nishi-ku, Niigata 950-2181, Japan
3. Department of Chemistry and Chemical Engineering, Faculty of Engineering, Niigata University, 8050 Ikarashi 2-Nocho, Nishi-ku, Niigata city, Niigata 950-2181 Japan; kano@eng.niigata-u.ac.jp
4. Department of Chemical System Engineering, Graduate School of Engineering, The University of Tokyo, Tokyo 113-8656, Japan; kmishima012@gmail.com
5. Center for Computational Sciences, Tsukuba University, Tsukuba 305-8577, Japan; mishima.kenji.fu@u.tsukuba.ac.jp
6. Department of Materials Science, Graduate School of Engineering Science, Akita University, Akita 010-8502, Japan; okawa@mine.akita-u.ac.jp

* Correspondence: kano@eng.niigata-u.ac.jp; Tel.:81-025-262-7218

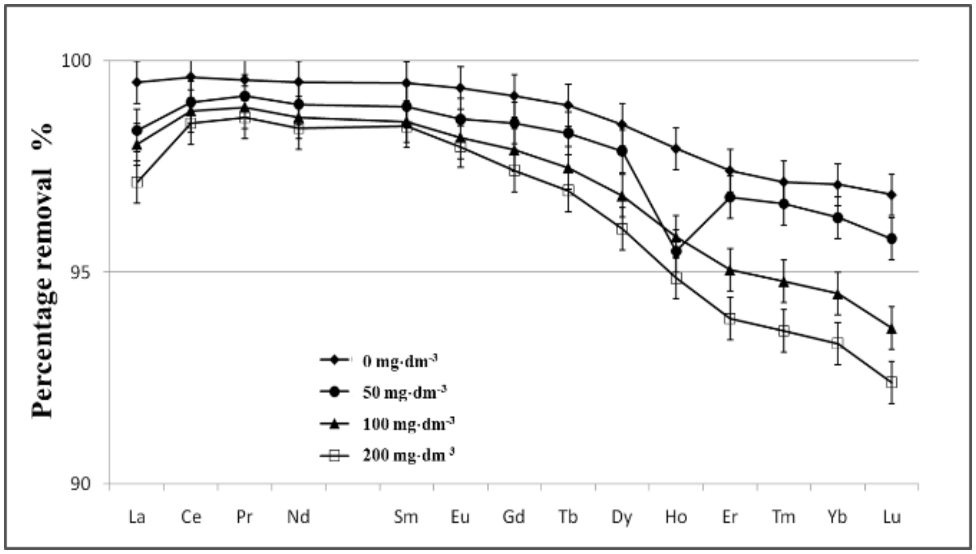

Figure S1. Effect of common ions (Ca^{2+}, Mg^{2+}, Na^{+} and K^{+}) on the removal efficiency of lanthanides using ground original sample.

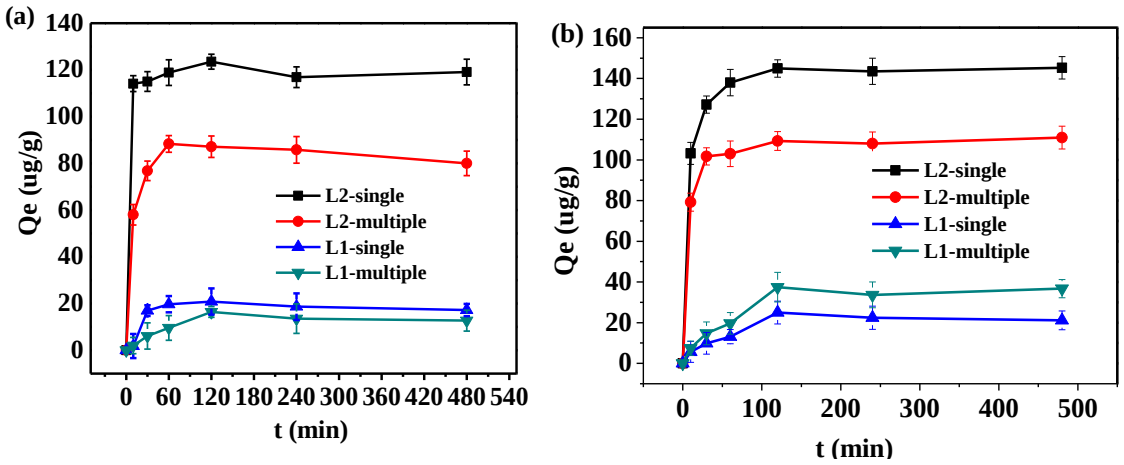

Figure S2. Adsorption capacity of (a) La(III) and (b) Eu(III) both in single and multiple solution by using L1 or L2.

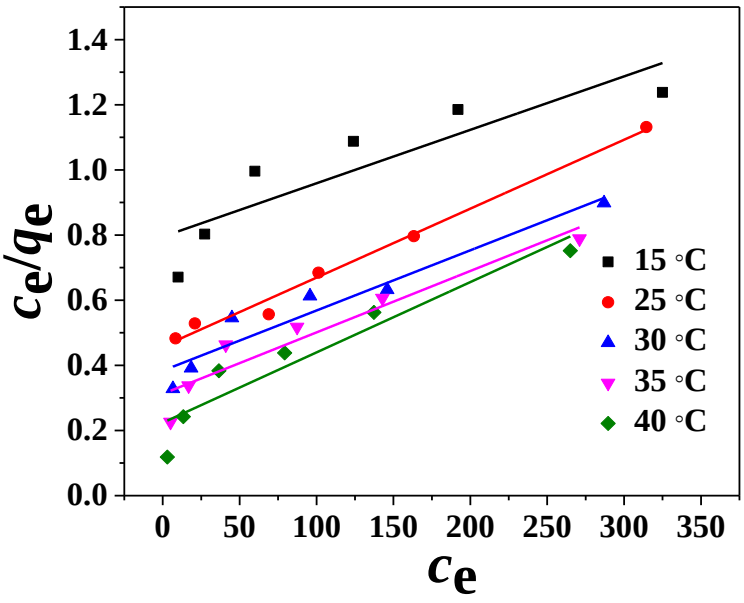

Figure S3. Langmuir isotherm for La(III) adsorption onto L2.

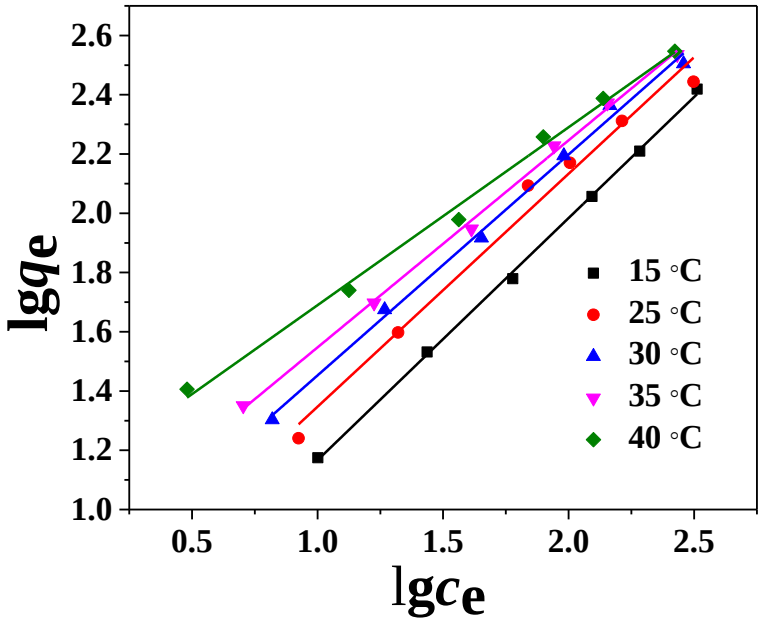

Figure S4. Freundlich isotherm for La(III) adsorption onto L2.

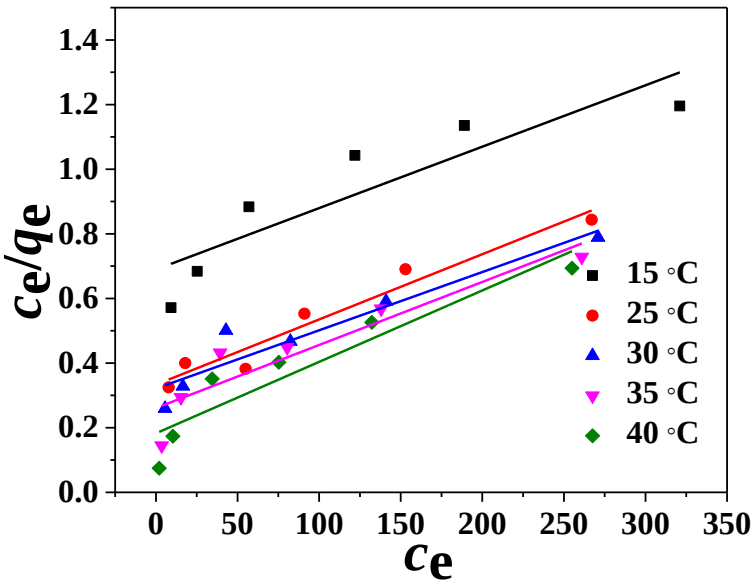

Figure S5. Langmuir isotherm fitting for Eu(II) adsorption onto L2.

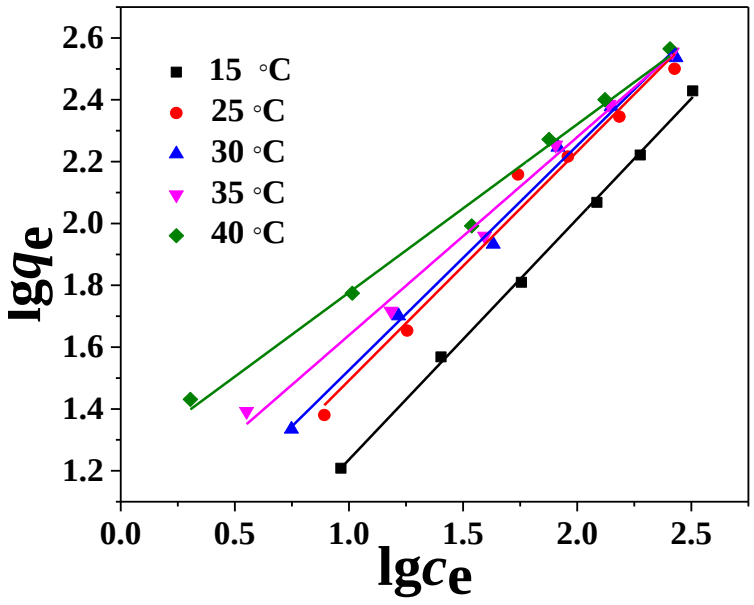

Figure S6. Freundlich isotherm fitting for Eu(III) adsorption onto L2.

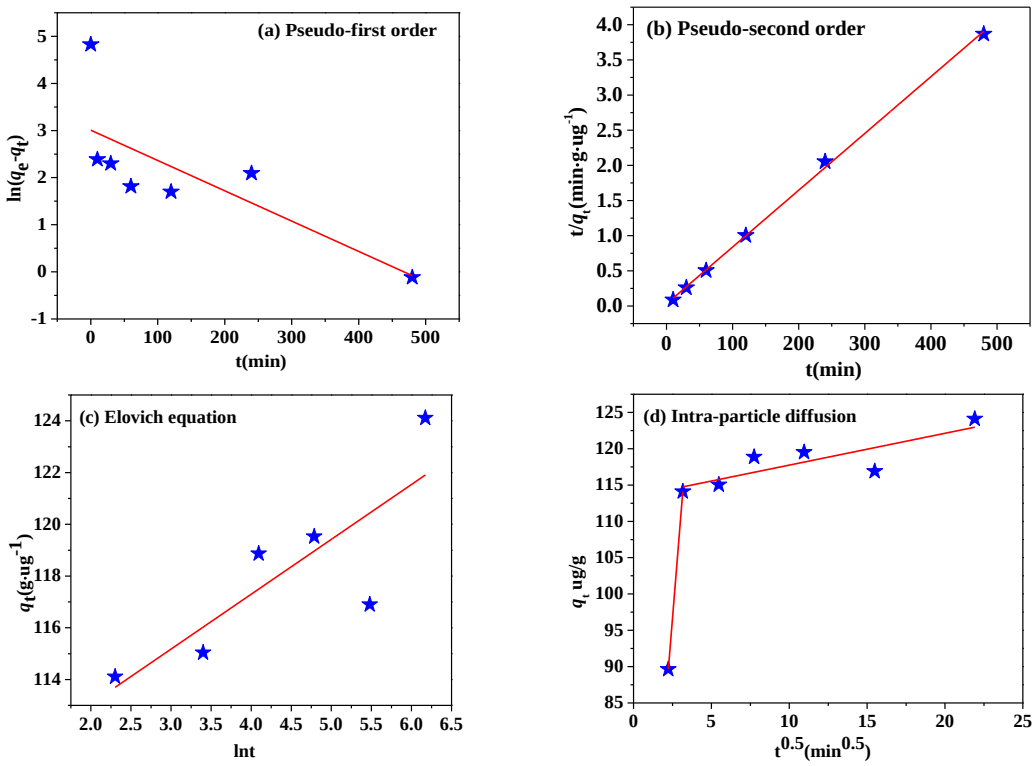

Figure S7. The kinetic models for La(III) adsorption onto L2.

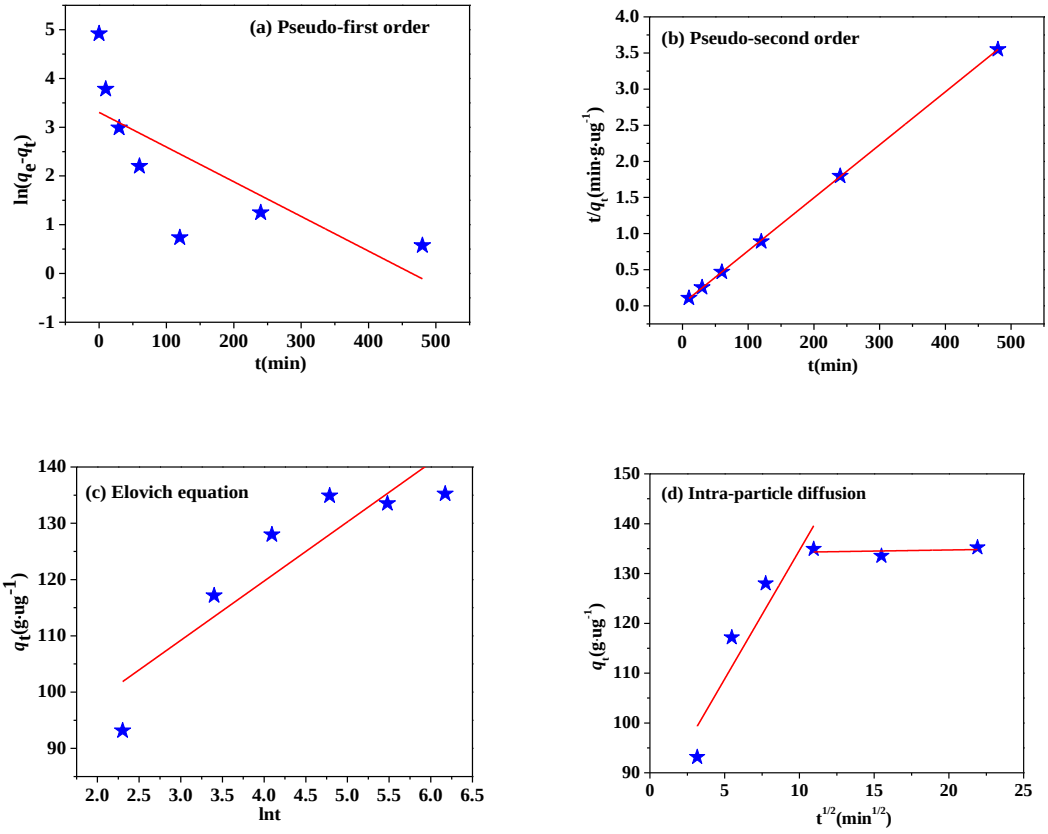

Figure S8. The kinetic models for Eu(III) adsorption onto L2.

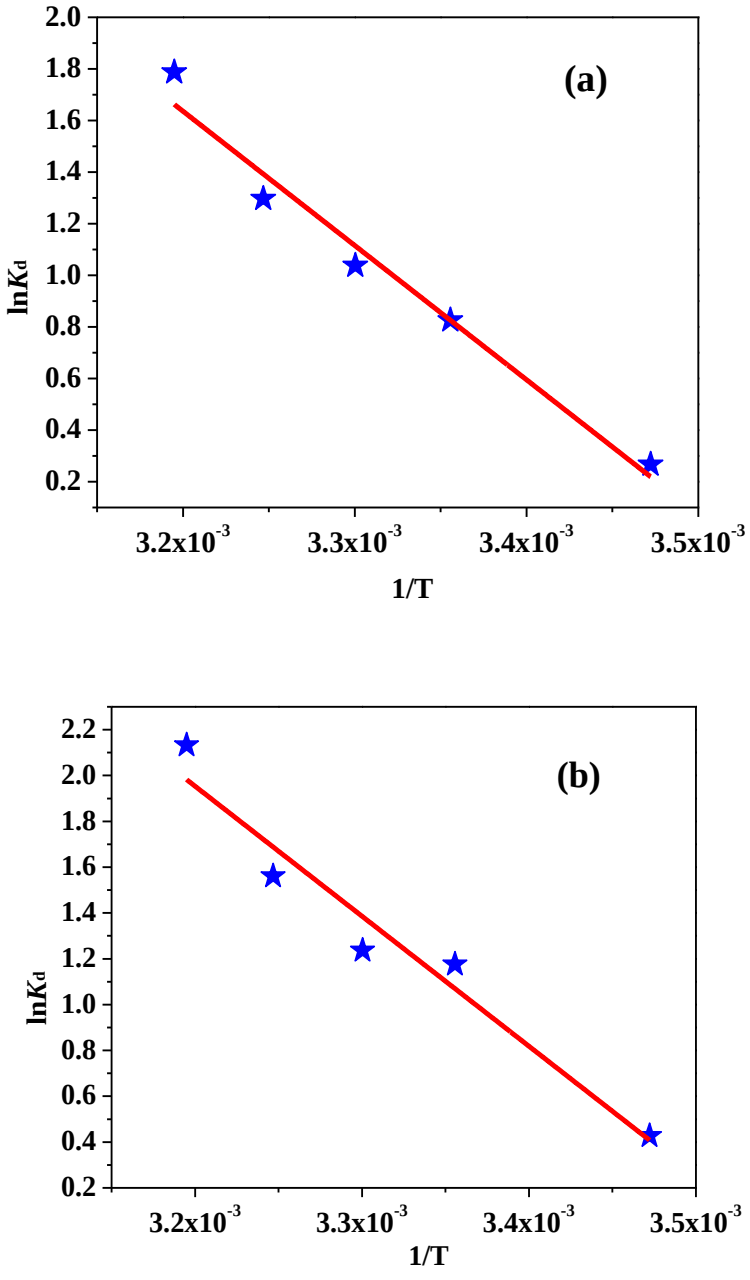

Figure S9. Plots of $\ln K_0$ vs. 1/T for the estimation of thermodynamic parameters obtained for the adsorption of (a) La(III) and (b) Eu(III) on L2.

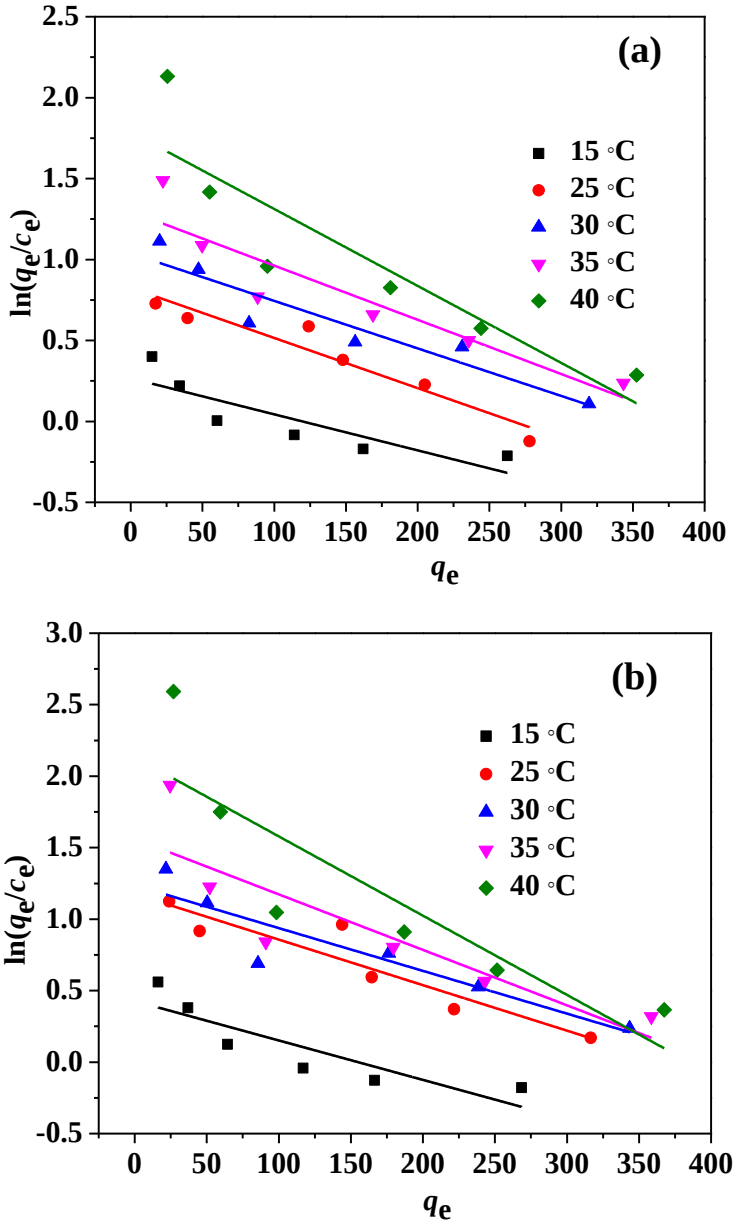

Figure S10. Plots of q_e vs. ln (q_e/c_e) for (a) La(III) and (b) Eu(III) on L2.

Table S1 Coefficients of Langmuir and Freundlich isotherms for La(III) adsorption onto L2.

Sample	Langmuir			Freundilich		
***T* (K)**	R^2	K_L(L μg^{-1})	q_{max}(μg g^{-1})	R^2	K_F	*n*
288	0.728	2.10X10^{-3}	610	0.999	2.24	1.22
298	0.986	4.60X10^{-3}	472	0.980	3.64	1.27
303	0.909	4.80X10^{-3}	541	0.995	5.09	1.34
308	0.885	6.00X10^{-3}	529	0.998	7.05	1.43
313	0.878	9.60X10^{-3}	463	0.994	12.3	1.67

Table S2 Coefficients of Langmuir and Freundlich isotherms for Eu(III) adsorption onto L2

Sample	Langmuir			Freundilich		
***T* (K)**	R^2	K_L(L μg^{-1})	q_{max}(μg g^{-1})	R^2	K_F	*n*
288	0.755	2.70X10^{-3}	526	0.998	2.23	1.28
298	0.940	6.10X10^{-3}	495	0.975	5.62	1.35
303	0.883	5.60X10^{-3}	556	0.991	6.28	1.38
308	0.830	7.10X10^{-3}	513	0.989	9.93	1.56
313	0.852	12.1X10^{-3}	452	0.988	16.9	1.84

Table S3 Kinetic parameters of Pseudo-first order and Pseudo-second order

Sample/T (298 K)	Pseudo-first order				Pseudo-second order		
	q_{exp} (μg g^{-1})	R^2	q_e (μg g^{-1})	K_1 (min^{-1})	R^2	q_{max} (μg g^{-1})	K_2 (g μg^{1}min^1)
La(III)	124	0.011	20.1	0.044	0.997	125	2.06X10^{-3}
Eu(III)	144	0.480	27.1	0.003	0.992	142	1.69X10^{-3}

Table S4 Kinetic parameters of Elovich model and Intraparticle diffusion

Sample/T (298 K)	Elovich model				Intraparticle diffusion		
	q_{exp} (μg g^{-1})	R^2	β (μg g^{1}min^{-1})	α (μg g^{-1}min^{-1})	K_{p1} (μg g^{-1}min$^{1/2}$)	K_{p2}	C_{ip} (μg g^{-1})
La(III)	124	0.604	1.39	1.96	26.4	113	30.6
Eu(III)	144	0.770	0.095	0.264	5.15	0.044	82.9

Table S5 Thermodynamic parameters for the adsorption of La(III) on L2.

T(K)	ΔH (kJ mol^{-1})	ΔS (J mol^{-1} K^{-1})	ΔG (kJ mol^{-1})
288	43.3	0.152	-0.637
298	-	-	-2.04
303	-	-	-2.61
308	-	-	-3.32
313	-	-	-4.63

Table S6 Thermodynamic parameters for the adsorption of Eu(III) on L2

T(K)	ΔH (kJ mol^{-1})	ΔS (J mol^{-1} K^{-1})	ΔG (kJ mol^{-1})
288	47.2	20.1	-1.02
298	-	-	-2.91
303	-	-	-3.11
308	-	-	-3.99
313	-	-	-5.55

The structural (in particular, the bond lengths) data and discussions on them are shown in Figure S11 and Tables S7-S10.

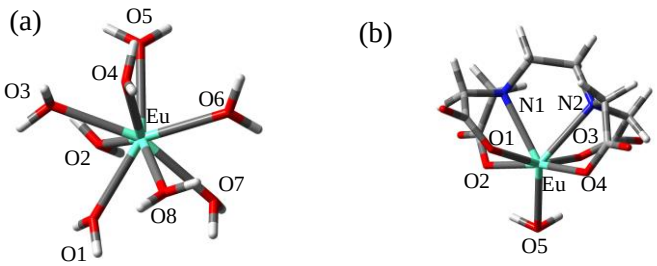

Figure S11. Optimized structures of (a) $[Eu(H_2O)_8]^{3+}$ and (b) $[Eu(EDTA)(H_2O)]^-$.

Table S7. Bond lengths of $[Eu(H_2O)_8]^{3+}$ shown in Panel (a) of Figure S11.

Bond	Bond length/Å
Eu-O1	2.40581
Eu-O2	2.45264
Eu-O3	2.46365
Eu-O4	2.45414
Eu-O5	2.46460
Eu-O6	2.43314
Eu-O7	2.50295
Eu-O8	2.42979
Avg.	2.45084

Table S7 shows the bond lengths between Europium and Oxygen atoms of $[Eu(H_2O)_8]^{3+}$ shown in Panel (a) of Figure S11. The bond lengths observed by EXAFS experimentally were reported to be 2.43 Å and 2.46 Å in 0.25 M HCl and 14.0 M LiCl, respectively [S1]. The average bond length shown in Table S8 is 2.45 Å, which is a good agreement with these experimental values.

Table S8. Bond lengths of $[Eu(EDTA)(H_2O)]^-$ in Panel (b) of Figure S11.

Bond	Bond length/Å
Eu-O1	2.28726
Eu-O2	2.39009
Eu-O3	2.34811
Eu-O4	2.29056
Eu-O5	2.59027
Avg. of Eu-O	2.38126
Eu-N1	2.61782
Eu-N2	2.61937
Avg. of Eu-N	2.61860

Table S8 shows the bond lengths between Europium and Oxygen or Nitrogen atoms $[Eu(EDTA)(H_2O)]^-$ in Panel (b) of Figure S11. Although there is no experimental result for this cluster, we find some tendencies from numerical results. First, the bond length, Eu-O5, in Panel (b) of Figure S11, is longer than any other Eu-O bond lengths. Second, the Eu-N bond lengths are longer than the bond Eu-O lengths.

Table S9. Bond lengths of $[Eu(H_2O)_8]^{3+}$ shown in Panel (a) of Figure S11.

Bond	Bond length/Å
Eu-O1	2.67716
Eu-O2	2.63467
Eu-O3	2.49634
Eu-O4	2.48377
Eu-O5	2.51739
Eu-O6	2.50596
Eu-O7	2.59509
Eu-O8	2.62578
Avg.	2.56702

Comparing Table S9 with Table S7, we can see that adsorption of the $[Eu(H_2O)_8]^{3+}$ complex on the hydrotalcite surface leads to the elongation of the Eu-O bonds.

Table S10. Bond lengths of $[Eu(EDTA)(H_2O)]^-$ in Panel (b) of Figure S11

Bond	Bond length/Å
Eu-O1	2.35931
Eu-O2	2.33345
Eu-O3	2.42208
Eu-O4	2.39675
Eu-O5	2.47791
Avg. of Eu-O	2.39790
Eu-N1	2.61747
Eu-N2	2.65364
Avg. of Eu-N	2.63556

Comparing Table S10 with Table S8, we can see that adsorption of the $[Eu(EDTA)(H_2O)]^-$ complex on the hydrotalcite surface also leads to the elongation of the Eu-O and Eu-N bonds in a similar way as comparing Table S9 with S7. But the degree of the elongation a little bit smaller for the former than the latter.

References

[S1] Allen et al., Inorg. Chem. 2000, 39, 595-601.